

Cosmic Ray Physics

DOMENICO D'URSO¹

*Istituto Nazionale di Fisica Nucleare (INFN), sez. Perugia
Via A. Pascoli, I-06123 Perugia, ITALY*

Cosmic ray story begins at the beginning of XX century. More than 100 years later, most of the main issues are still open questions, as sources, acceleration mechanism, propagation and composition. There is a continuing fascination with the studies of cosmic radiation mostly from the several contradictions connected to its observation. The radiation has an energy spectrum ranging from ~ 1 GeV to beyond 10^{20} eV with a flux going from 1 particle per m^2 per μs to less than 1 particle per km^2 per century, and so very different experimental techniques are needed to perform cosmic ray measurements in the different energy intervals. In this contribution the actual experimental status of cosmic ray knowledge will be reviewed.

PRESENTED AT

XXXIV Physics in Collision Symposium
Bloomington, Indiana, September 16–20, 2014

¹Work supported by the Istituto Nazionale di Fisica Nucleare (INFN).

1 Introduction

The Earth's atmosphere is continuously bombarded by extraterrestrial particles, the so called Cosmic Rays (*CR*), which consist of ionized nuclei, mainly protons, alpha particles and heavier nuclei. Most of them are relativistic and a few particles have an ultrarelativistic kinetic energy, extending up to 10^{20} eV.

CR story starts at the beginning of the 20th century when it was found that electroscopes discharged even in the dark, well away from sources of natural radioactivity. To solve the puzzle, in 1912 Hess [1] and successively Kolhörster [2] made a series of manned balloon flights, in which they measured the ionization of the atmosphere with increasing altitude.

From *CR* studies the elementary particle physics was born. Indeed, from cosmic radiation track studies with cloud chamber, Blackett and Occhialini [3] in 1933 discovered the positron and in 1936 Anderson and Neddermeyer [4] announced the observation of particles with mass intermediate between that one of the electron and the proton, the muon. With a new kind of instrument, nuclear emulsion, in 1947 there was the observation of the pion by Rochester and Butler [5] and so on till the Σ particle discovery in 1953 [6].

As testified from their history, *CR* could be messenger of new physics and yet unknown particles. They are messengers of astrophysical sites, even the most powerful ones. Via *CR* studies it is possible to infer the properties of cosmic environment through which they propagate. Furthermore, they are the only window on very high energy phenomena, well far from LHC energy scale, and can be use to verify standard physical laws, as the Lorentz invariance, in extreme conditions.

After more then 100 years of studies, most of the main related issues are still open questions, as sources, acceleration mechanism, propagation and composition. These opened issues are a puzzle still today, whose solution involves astronomy and cosmology, nuclear physics and elementary particle physics.

2 Cosmic Ray Physics Case

The most striking feature of cosmic rays is their energy spectrum, which spans a very wide range of energies with surprising regularity. As it is possible to see in fig. 1, the differential flux of the all-particle spectrum goes through 32 orders of magnitude along over 12 energy decades. The regularity is broken only in few regions: the *knee* at about 3×10^{15} eV, the *second knee* at about 4×10^{17} , the *ankle* at about 4×10^{18} eV and the *suppression* at the highest energies. Except a “saturation” region at low energies, cosmic ray spectrum can be well represented by power-law energy distribution

$$\frac{dN}{dE} \sim E^{-\gamma} \quad (1)$$

where $\gamma \sim 2.7$ up to the *knee*, then ~ 3.0 up to the *second knee* where it becomes ~ 3.3 up to the *ankle*. Beyond the *ankle*, the spectrum can be described with a γ value of ~ 2.6 up to the *suppression* region ($\sim 3 \times 10^{19}$).

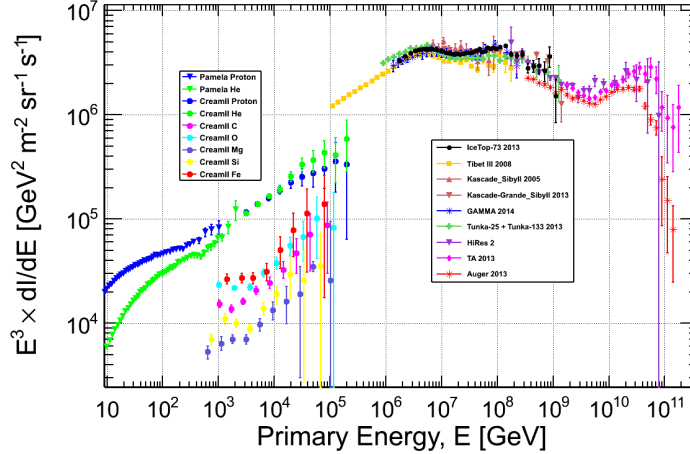


Figure 1: All-particle energy spectrum from a compilation of measurements of the differential energy spectrum of *CR* multiplied by E^3 to enhance spectrum structures.

Below the *knee*, cosmic radiation is believed to originate within the galaxy and accelerated by supernovae explosion. As measured by direct experiments, $\sim 99.8\%$ of *CR* are charged particles and only $\sim 0.2\%$ are photons and neutrinos. 99% of charged particles are nuclei and 1% are electrons and positrons. Among the nuclei, protons are $\sim 87\%$, helium nuclei $\sim 12\%$ and heavier nuclei $\sim 1\%$. Relative abundances are quite similar to those measured from the Solar System. The differences can be explained as result of spallation processes of primary particles propagating through the interstellar matter: excess of lithium, beryllium and boron nuclei; excess of elements just less heavy than those of the iron group. In a standard scenario, where primary particle acceleration and propagation is due to magnetic fields (effects depend only on rigidity), the *knee* is explained as the limit at which galactic magnetic field can no more confine cosmic particles: each radiation component is expected to have a *knee* corresponding to the rigidity at which it can be no more confined, from the lightest, protons and helium nuclei, to the heaviest ones. In this scenario, the *knee* is explained as the escaping limit of the light component of *CR*. Recent experiments are pushing a new light on this region of the spectrum, with unprecedented precision measurements of particle spectra. When it is not possible to perform direct measurements of primary particles (typically for $E_{primary} > 10^{14}$ eV), the radiation

composition is inferred from indirect observations. Then conclusions are strongly dependent on models used to describe the data. Different methods used for mass measurement usually give different answers.

As already anticipated, most of the main questions about *CR* are still open: origin, composition and acceleration and propagation mechanisms. Nowadays the *CR* community is focusing on the following issues:

- particle abundances below the knee, searching for any hint of new physics;
- connection between direct and indirect observations;
- nature of spectrum features (knee, ankle,...);
- galactic to extragalactic transition;
- nature of the spectrum suppression at the highest energies.

Cosmic radiation of energy up to 10^{14} eV could be studied directly by detection of primary particle by means of balloon and satellite experiments. Going up with the energy, *CR* flux becomes too low to use direct detection, since it is impossible to employ wide area detectors on balloons or in the space. Above 10^{14} eV *CR* have enough energy to initiate a cascade by interacting with the atmosphere, whose products are detected at ground. At those energies, *CR* are investigated through the observation of these extensive air showers (EAS), using particle detectors, at ground, of suitable area to measure shower front and lateral distribution, the sampling and the extension of the apparatus depend on the energy region one is interested in.

The direct detection allows to perform a particle identification and to have the energy scale of the detector fixed by calibration at ground. The limit of measurement is the size of possible detectors and consequently the limited energy range. In the case of indirect measurements, it is possible to measure *CR* up to 10^{20} eV but all the measurements are based on modelling interactions of primary *CR* with the atmosphere.

3 Direct Measurements

Direct measurements are performed by stratospheric balloons or space experiments. In the last decades, direct experiments on cosmic rays received a push forward by the possibility of conducting experiments on board of long duration balloon flights, satellites and on the International Space Station. The increase in the collected statistics and the technical improvements in the construction of the detectors allows to measure the fluxes at higher energies with a reduced discrepancy among different experiments respect to the past. Due to the statistics of particle flux, the sensitivity

of different experiments are determined by the combination of detector livetime and acceptance. Balloon experiments usually have a larger acceptance but a shorter livetime, while space experiments can have a larger livetime but a reduced detector size due to size/weight limits imposed by space mission constraints. In the last years there were no updates from balloon experiments. For a review of direct measurements of CR by balloon experiments one can refer to [7].

Recently important observations have been reported about the proton and helium spectrum by PAMELA [8] and by AMS-02 [9] about the electron and positron spectra. In the following the two detectors will be described and their main results discussed.

3.1 PAMELA and AMS-02 experiments and results

PAMELA (Payload for Antimatter Matter Exploration and Light-nuclei Astrophysics) is a satellite-borne experiment designed to study charged particles in the cosmic radiation. A schematic view of the apparatus is shown in fig. 2. The central part of the apparatus is a magnetic spectrometer, consisting of a permanent magnet and a 6 double layer of silicon detector planes to measure the rigidity and the ionisation energy losses, dE/dx . Below the spectrometer an electromagnetic calorimeter (ECAL) is installed to measure energy particle and to perform particle identification. The apparatus is equipped with a Time of Flight (ToF) system of plastic scintillators for the trigger, with a capability of 12 independent measurements of particle velocity, $\beta = v/c$. The ToF allows to discriminate between down-going and up-going particle, enabling the spectrometer to determine the sign of the particle charge, and 6 independent dE/dx measurements. There is also an anticoincidence system to identify in the offline analysis apse triggers and multi-particle events corresponding to secondary particles produced in the detector. In the bottom part of the apparatus, there is a neutron detector (ND) that detects the neutron production associated with hadrons to increase the electron-proton discrimination.

The AMS-02 (Alpha Magnetic Spectrometer) is a general purpose high energy particle physics detector installed on the International Space Station. The layout of AMS-02 detector is shown in fig 3. It consists of nine planes of precision silicon tracker, a transition radiation detector (TRD), four planes of time of flight counters (TOF), a permanent magnet, an array of anticoincidence counters (ACC), placed around the inner tracker, a ring imaging Čerenkov detector (RICH) and an electromagnetic calorimeter (ECAL) of 17 radiation lengths. The figure also reports a high-energy electron of 1.03 TeV detected by AMS. The tracker accurately determines the trajectory and absolute charge (Z) of particles. The TRD is designed to use transition radiation to distinguish between e^- and protons, and dE/dx to independently identify nuclei. The coincidence of signals from all of the four ToF planes provides a charged particle trigger for the apparatus. The ACC system around the magnet and the inner tracker allow to reject events corresponding to particles entering or leaving

the inner tracker volume transversely. The RICH is designed to have an independent measurement of the magnitude of the charge of cosmic rays and their velocities with a precision of $\Delta\beta/\beta \sim 1/1000$. The ECAL allows to measure particle energy and it provides an independent discrimination between electrons and protons.

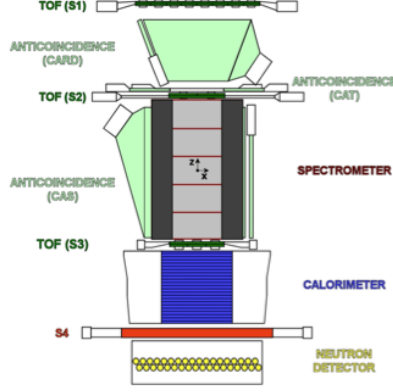


Figure 2: Schematic view of the PAMELA apparatus.

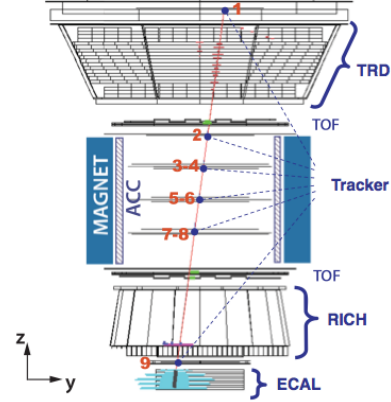


Figure 3: Schematic view of the AMS-02 apparatus traversed by a 1.03 TeV electron event.

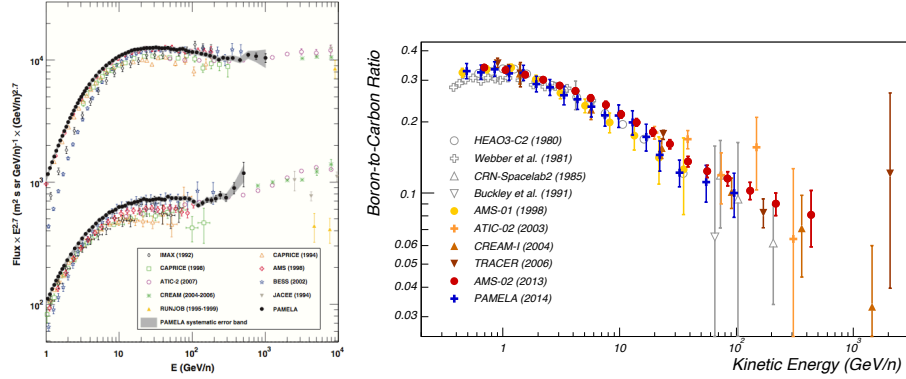


Figure 4: Proton and helium absolute fluxes (left plot) measured by PAMELA [10] above 1 GeV per nucleon and boron-to carbon flux ratio (right plot) measured by PAMELA [15] and AMS-02 [16]. Results from previous measurements [11] [17] are also shown.

Protons and helium nuclei are the most abundant *CR* species and hence they allow to understand the detector limits in terms of tracker resolution and systematic uncertainties. Recently a measurements of proton and helium spectra has been published by PAMELA [10]. In the left plot of fig. 4 proton and helium fluxes are shown

multiplied by a power of the energy, $E^{2.7}$, to enhance spectral features, compared with a few of previous measurements. In this energy region, in a scenario based on a shock diffusion acceleration model and a diffusive propagation in the Galaxy [12], the spectrum is expected to have a featureless behaviour and to be well fitted by a single power law with similar spectral indices for protons and heavier nuclei. For energy greater than 30 GV (above the influence of solar modulation), PAMELA observed a different spectral shape for proton and helium spectra. Furthermore data can not be described by a single power law model, a change in the spectral index has been observed around 200 GV (the single power law hypothesis is rejected at the 95 % confidence level). The measured spectral indices are $\gamma_{1p} = 2.85 \pm 0.015(\text{stat}) \pm 0.004(\text{sys})$ and $\gamma_{1\text{He}} = 2.766 \pm 0.01(\text{stat}) \pm 0.027(\text{sys})$ below 230 GV for protons and helium nuclei respectively, while they become $\gamma_{2p} = 2.67 \pm 0.03(\text{stat}) \pm 0.05(\text{sys})$ and $\gamma_{2\text{He}} = 2.48 \pm 0.06(\text{stat}) \pm 0.03(\text{sys})$ above 230 GV. Those observations challenge the “standard” scenario: models do not reproduce data across the full-rigidity region and they do not predict a significant difference between proton and helium indices. New features could be interpreted as an indication of different population of *CR* sources [13] or of a new physical phenomenon in the propagation [14] .

The relative abundances of *CR* species provide information about cosmic-ray transport within the Galaxy: *CR* such as carbon and oxygen may interact with the interstellar medium to produce secondary fragments such as lithium, beryllium and boron. The ratio of secondary to primary *CR* can be used to estimate the amount of traversed interstellar matter. One of the most sensitive quantities is the ratio of boron to carbon, because boron is purely secondary and its main progenitors carbon and oxygen are primaries. The shape of this ratio is highly sensitive to propagation coefficients. Due to their similar charge, the B/C ratio is the less affected by systematics or solar modulation. Recently PAMELA and AMS-02 reported a measurement of B/C ratio flux [15] [16]. In the right plot of fig. 4 the B/C ratio as a function of kinetic energy per nucleon measured by PAMELA and AMS-02 is shown with data of previous experiments. New data fix tighter constraints for propagation models. Anyway, at high energy, the main limitation for the ratio measurement is the statistics but AMS has collected only 10% of the expected statistics. The B/C behaviour at high energy will become more clear with more data.

Electrons and positrons are only $\sim 1\%$ of cosmic radiation but they provide important information regarding the origin and propagation of *CR*. In the last months AMS-02 published the measurements of positron and electron fluxes [18] and an update of positron fraction [19], fixing the limit of present knowledge of electron/positron radiation component .

The positron fraction is defined as the ratio of the positron flux to the combined flux of positrons and electrons. In fig. 5 the measured positron fraction by AMS-02 is presented as a function of the energy, compared with previous measurements, from 1 to 35 GeV (left plot) and from 10 to 500 GeV (right plot). As expected from diffuse

positron production, there is a rapid decrease from 1-8 GeV. From 10 to 200 GeV a steadily increasing has been confirmed and above 200 GeV the fraction seems to flatten out. An Upper limit on dipole anisotropy amplitude $d \leq 0.030 @ 95\% \text{CL}$ ($E > 16$ GeV) has been also reported. In this scenario, the measurement of the *end* of positron fraction will be crucial to understand the nature of the positron excess.

In fig. 6 are shown the separated flux for electrons and positrons measured by AMS-02, from 0.5 to 700 GeV and from 0.5 to 500 GeV respectively. Neither the electron flux nor the positron flux can be described by single power laws over the entire range. Above ~ 20 GeV and up to 200 GeV the electron flux decreases more rapidly with energy than the positron flux, that is, the electron flux is softer than the positron flux. This is not consistent with only the secondary production of positrons [20]. So the rise in the positron fraction seems to be due to the hardening of the positron spectrum and not to the softening of the electron spectrum.

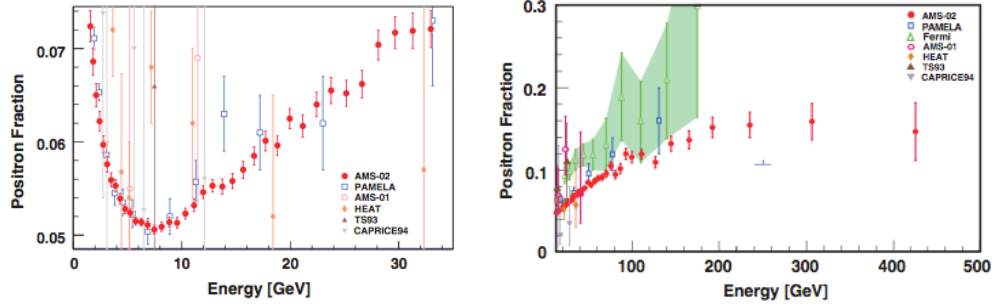


Figure 5: AMS-02 positron fraction from 1 to 35 GeV (left) and from 10 to 500 GeV, compared with previous measurements.

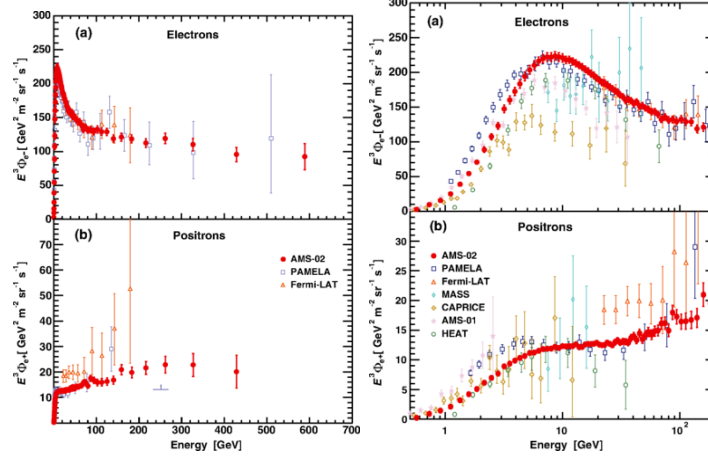


Figure 6: Global (left plot) of AMS-02 (a) electron, from 0.5 to 700 GeV, and (b) positron fluxes, from 0.5 to 500 GeV, multiplied by E^{-3} . In the right plot a detailed view from 0.5 to 200 GeV is shown. Also shown are data from previous experiments.

4 Indirect Measurements

The indirect measurements of CR are based on the observation of EAS observables: particles at ground, like electrons, nucleons and hadrons; Čerenkov light, used in the energy range 10^{14} - 10^{16} eV; fluorescence light, used for energies higher than 10^{17} eV. Recently has been proven also the possibility of using radio signals. The main issue of CR detected by means of indirect techniques is the understanding of the EAS generated by a primary particle whose energy is estimated to exceed 10^{18} eV (Ultra High Energy Cosmic Rays, UHECR). In the last years, new results have been published about the energy spectrum, the mass composition and the distribution of arrival directions of primary particles by the Auger [21] and the Telescope Array (TA) [22] experiments. In the following Auger and TA experiments will be described and their results will be discussed. For a history and a complete review of CR indirect detection techniques one can refer to [23, 24].

4.1 Auger and TA experiments and results

The two experiments are the last UHECR generation experiments, based on the use of an *hybrid* detection technique: a combined use of a surface detector (SD) and of a nitrogen fluorescence detector (FD). Employing two complementary techniques to observe EAS, SD and FD are able to perform independent measurements on the same shower: the lateral and temporal distribution of shower particles at the ground level with SD, the air shower development in the atmosphere (the longitudinal profile) above the surface array with FD. Both techniques have limits and advantages. FD allows to have a nearly calorimetric energy measurement, with a direct view of shower evolution, but it has only 15% of duty cycle and its acceptance grows up with energy and depends on atmosphere conditions. SD has a duty cycle of 100% and an acceptance flat above threshold, but its estimation of primary energy is based on Monte Carlo studies.

The use of two detection techniques allows to have: an inter-calibration of the two methods, to study their systematic uncertainties; an energy spectrum estimation almost model independent; an enhanced composition sensitivity, FD directly measures the depth at which the shower reaches its maximum (X_{max}) while SD measures particle densities and time width of the shower front at ground level, all fingerprints of primary's nature.

The Southern Observatory is located in the Pampa Amarilla upland. The SD of the Pierre Auger Observatory [25] consists of 1600 water Cherenkov tanks on a regular hexagonal grid with a distance of 1500 m between tanks, covering a total area of 3000 km². At an altitude of 1400 m above sea level, corresponding to a vertical atmospheric depth of 875 g cm⁻², The area is overlooked by 4 fluorescence detectors (eyes) [26], disposed at the edges of the surface array.

TA is located in the high desert in Millard County, Utah. It consists of a SD of more then 500 scintillator detectors disposed on a 1.2 km square grid, covering 700 km² The area is overlooked by 3 telescope stations.

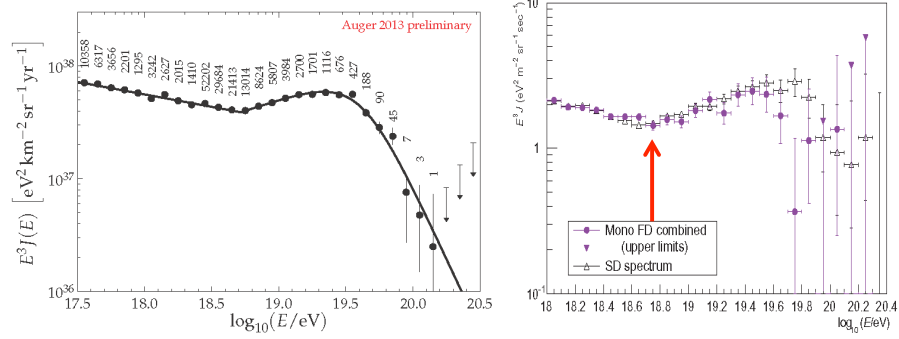


Figure 7: Energy spectrum as measured at the Pierre Auger Observatory (left) and by the Telescope Array experiment (right) using the Mono FD combined and the SD measurements. In the case of Auger, numbers give the total number of events inside each bin and the last three arrows represent upper limits at 84% CL, for TA upper limits are given at 68% CL.

Recent measurements of energy spectrum have been reported by the Pierre Auger observatory at the ICRC 2013 [27] and by the TA experiment [28] (see fig. 7). The Auger Collaboration presented an update of his spectrum measurement, combining the hybrid spectrum (hybrids events) with the SD spectrum (SD events whose energy has been calibrated with FD), covering the range from $10^{17.5}$ to $10^{20.5}$ eV. To characterize the spectral features data have been described with a simple power law below the ankle, 5×10^{18} eV and a power law with smooth suppression above. The obtained spectral index above the ankle is $3.23 \pm 0.01(\text{stat}) \pm 0.07(\text{sys})$ and $2.63 \pm 0.02(\text{stat}) \pm 0.04(\text{sys})$ above. The suppression is seen with a significance of 20σ . The TA Collaboration presented a measurement FADC-based FDs in monocular mode, from 10^{18} to $10^{20.2}$ eV TA identify the ankle at $10^{18.75}$ eV and a spectrum suppression at $10^{19.50}$ eV with a significance of 3.2σ . Experiments have a difference in their energy scale of about 14%, compatible with their systematic (14% for Auger and 21% for TA). Both confirm the spectrum structures of ankle and the suppression, however their origin is yet to be determined. These features can originate from the interaction of primaries with the CMB: attenuation due to pair production can explain the ankle and pion production from protons-CMB interactions or photo-disintegration of nuclei can produce the suppression. Alternatively, the structures derive from the spatial distribution of sources and their acceleration mechanism. In that case the ankle could identify the transition point from a galactic dominated radiation to an extra-galactic dominated one. Several scenarios have been put forward to explain the spectrum (for an overview see [29]).

Important part of this puzzle is the mass composition measured in this energy range. The Pierre Auger Collaboration reported [30] an update of the evolution with energy of the first two moments of the X_{max} distributions. As one can see from left plot of fig. 8, Data clearly indicate a change of behaviour at a few EeV, i.e. in the Ankle region. Under the hypothesis that no new interaction phenomena in the air shower development come into play, the data clearly support the hypothesis of a mass composition evolving in the Ankle region. In the case of TA data, see right plot in fig. 8, a light, nearly protonic, composition is in good agreement with the data, in the whole energy range. Detailed comparison of the two measurements and of the two analysis techniques to understand the mutual differences [32].

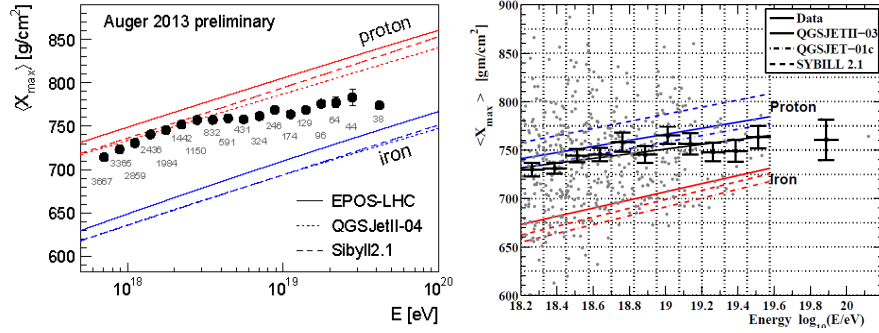


Figure 8: Evolution of $\langle X_{max} \rangle$ as a function of the energy measured by the Pierre Auger Observatory (left) and the Telescope Array experiment (right) compared with simulation expectations.

The observation of structures in the arrival direction distribution of primaries is also related to the mass of the radiation, it changes the angular scale at which a possible correlation could be observed, and directly to the origin of the radiation (Are there nearby sources?) Searches of possible anisotropy have been done by both hybrid experiments. In particular, the Pierre Auger Collaboration claimed a possible correlation between the distribution of arrival directions and an AGN catalogue [33]. Auger Collaboration found evidence of anisotropy in the arrival directions of cosmic rays above the Greisen-Zatsepin-Kuz'min energy threshold, 6×10^{19} eV. The anisotropy was measured by the fraction of arrival directions that are less than 3.1° from the position of an active galactic nucleus within 75 Mpc (using the Véron-Cetty and Véron 12th catalog). In their last publication on the subject [34], with 69 events with energy greater than 55 EeV, they reported a degree of correlation of $38^{+7}_{-6}\%$, against a 21% expected in the hypothesis of an isotropic flux. Furthermore, an excess around Cen A has been observed, 18.8 % of events lie within 18° from the source, while 4.7% is expected from an isotropic flux. A cluster of arrival direction has been observed also by the TA experiment [35]. Using CR with energy greater than 57 EeV (87 events), they found a cluster centred at (R.A.=146.7°, decl.=43.2°), with a

statistical significance of 5.1σ . They also estimated the probability of such a hotspot to appear by chance in an isotropic sky to be 3.7×10^{-4} .

5 Discussion and conclusions

After more then 100 hers of studies and experiments, the understanding of cosmic radiation is still a puzzle to be solved.

In the last decades, direct experiments on cosmic rays received a push forward by the possibility of using long duration balloon flights, satellites and on the International Space Station. The increase in the collected statistics and the technical improvements of apparatus of the most recent experiments offered the opportunity to have very important results on the cosmic radiation, especially from space-borne experiments. Accurate measurements of positron fraction and of electron and positron fluxes have been performed. A clear positron excess has been established from 10 to 200 GeV. AMS-02 Collaboration has observed a flattening above 200 GeV and only the determination of the *end* of the excess will help to understand the nature of the excess and if is an indirect sign of dark matter. Detailed measurements of proton and helium spectra from PAMELA Collaboration show several unexpected features: different spectral indices for the primaries and a change of the spectral index around 240 GeV for both. Only a more accurate measurement will clarify the existence of those structures (AMS-02 results are expected by the beginning of 2015). A very accurate measurement of boron-to-carbon ratio has been performed by the AMS-02 and PAMELA Collaborations, putting tighter constraints on propagation models of *CR* in the Galaxy. While PAMELA experiment is over, AMS-02 will take data till the decommissioning of the International Space Station. In the present AMS-02 publications only 10% of the total available statistics is used, hence mayor contributions are expected from AMS-02 in the future. Furthermore, there are several new space based experiments that will be installed on the ISS, that will become a kind of *CR* Observatory. Those experiments will extend the energy range of direct measurements of galactic *CR*, leading to the connection between direct and indirect observations.

At higher energies, a full explanation of all spectral features is still missing. The last generation of UHECR experiments, the Auger Observatory and Telescope Array experiment, confirm the *end* of the spectrum but its nature is unclear. There is still to be understood if there is a transition from a galactic dominated radiation to an extra-galactic dominated one and if it occurs at which energy and in which way. Spectral features could originate from the interaction of primaries with the CMB, then suppression would be explained in a GZK-scenario. Or they could derive from the distribution of sources and their acceleration mechanism and in that case the suppression would be explained in a source-scenario. UHECR mass composition is still an open issue and data reported from Auger and TA Collaborations are not in agreement. For

the future there are many upgrades planned for Telescope Array experiment and the Auger Observatory to understand the origin of the flux suppression, to identify the proton contribution at the highest energies and to improve comprehension of EAS development.

References

- [1] V. Hesse, Phys. Zeit **13**, 1084 (1912).
- [2] W. Kolhörster, Phys. Zeit, **14**, 1153 (1913).
- [3] P. Blackett, G. Occhialini, Proc. Roy. Soc., **A139**, 699 (1933).
- [4] C.D. Anderson, S. Neddermeyer, Phys. Rev., **51**, 884 (1937).
- [5] G.D. Rochester, C.C. Butler, Nature **160**, 855 (1947).
- [6] A. Bonetti, R. Levi-Setti, M. Panetti, G. Tomasini, Nuovo Cim., **10**, 345 (1953).
- [7] E.S. EO, Astropart. Phys., **39-40**, 76 (2012).
- [8] O.Adriani et al., “The PAMELA Mission: Heralding a new era in precision cosmic ray physics” Physics Reports, **544**, 323-370 (2014).
- [9] M. Aguilar et al., Phys. Rev. Lett., **110**, 141102 (2013).
- [10] .O.Adriani et al., Science, **332**, 69 (2011).
- [11] J. P. Wefel et al., in Proceedings of the 30th International Cosmic Ray Conference, R. Caballero et al., Eds. (Universidad Nacional Autonoma de Mexico, Mexico City, 2008), **2**, pp. 3134; H. S. Ahn et al., Astrophys. J. Lett. **714**, L89 (2010); K. Asakimori et al., Astrophys. J. **502**, 278 (1998); M. Hareyama, RUNJOB collaboration, J. Phys. Conf. Ser. **31**, 159 (2006); W. Menn et al., Astrophys. J. **533**, 281 (2000); M. Boezio et al., Astrophys. J. **518**, 457 (1999); M. Boezio et al., Astropart. Phys. **19**, 583 (2003); S. Haino et al., Phys. Lett. B **594**, 35 (2004); AMS Collaboration, Phys. Lett. B **490**, 27 (2000).
- [12] A. W. Strong, I. V. Moskalenko, V. S. Ptuskin, Annu. Rev. Nucl. Part. Sci., **57**, 285 (2007).
- [13] S. Thoudam, JR Horandel, Mon Not R Astron Soc, **421**, 12091214 (2012); S. Thoudam, JR Horandel, “Revisiting the hardening of the cosmic-ray energy spectrum at TeV energies”, arXiv:1304.1400 (2013).
- [14] N. Tomassetti, Astrophys J Lett, **752**, (1) L13 (2012).

- [15] Adriani et al., ApJ **791**, 93 (2014).
- [16] A. Oliva et al., Proceeding of 33rd ICRC (2013).
- [17] J.J. Engelmann et al., A&A 233, 96 (1990); W. R. Webber et al., Proceeding of 19th ICRC (1985); D. Muller et al., ApJ **374**, 356 (1991); J. Buckley et al., ApJ **429**, 736 (1994); M. Aguilar et al., ApJ **724**, 328 (2010); A.D. Panov et al., Proceeding of 30th ICRC (2008); H.S. Ahn et al., APh **30**, 133 (2008); A. Obermeier et al., ApJ **752**, 69 (2012).
- [18] M. Aguilar et al. (AMS Collaboration), Phys. Rev. Lett. **113**, 121102 (2014)
- [19] M. Aguilar et al. (AMS Collaboration), Phys. Rev. Lett. **113**, 121101 (2014)
- [20] P.D. Serpico, Astropart. Phys. **39-40**, 2 (2012).
- [21] Abraham J, et al. Nucl. Instrum. Methods A **523**,50 (2004)
- [22] Abbasi R, et al., Proceeding of 30th ICRC (2007).
- [23] M. Nagano, A.A. Watson, Rev. Mod. Phys. **72**, 689 (2000)
- [24] K.H. Kampert, A.A. Watson, arXiv: 1207.4827 (2012).
- [25] Allekotte I, et al., Nucl. Instr. Methods A **586**, 409 (2008).
- [26] J. Abraham et al., Nucl. Instr. Methods A **620**, 227 (2010).
- [27] A. Schulz et al., Proceeding of 33rd ICRC (2013).
- [28] T. Abu-Zayyad et al., Astropart. Phys. **48**,16 (2013).
- [29] A. Letessier-Selvon and T. Stanev, Rev. Mod. Phys. **83**, 907 (2011).
- [30] Letessier-Selvon et al., Proceeding of 33rd ICRC (2013), arXiv:1310.4620.
- [31] Abbasi et al., arXiv:1408.1726v1.
- [32] T. Abu-Zayyad, et al., Pierre Auger Observatory and Telescope Array: Joint Contributions to the 33rd International Cosmic Ray Conference (ICRC 2013)arXiv:1310.0647.
- [33] The Pierre Auger Collaboration, Science **318**, 938 (2007).
- [34] P. Abreu et al. , Astropart. Phys., **34** 314 (2010).
- [35] R. Abbasi et al., Ap. J (Lett) **790**, L21 (2014).